Draft version September 27, 2016
Preprint typeset using LaTeX style emulateapj v. 5/2/11

arXiv:1609.07510v1 [astro-ph.EP] 23 Sep 2016

WIND-DRIVEN ACCRETION IN TRANSITIONAL PROTOSTELLAR DISKS

Lile Wang[1] and Jeremy J. Goodman[1]

Draft version September 27, 2016

ABSTRACT

Transitional protostellar disks have inner cavities heavily depleted in dust and gas, yet most show signs of ongoing accretion, often at rates comparable to full disks. We show that recent constraints on the gas surface density in a few well-studied disk cavities imply that the accretion speed is at least transsonic. We propose that this is the natural result of accretion driven by magnetized winds. Typical physical conditions of the gas inside such cavities are estimated for plausible X-ray and FUV radiation fields. The gas is molecular and predominantly neutral, with a dimensionless ambipolar parameter in the right general range for wind solutions of the type developed by Königl, Wardle, and others. That is to say, the density of ions and electrons is sufficient for moderately good coupling to the magnetic field, but not so good that the magnetic flux need be dragged inward by the accreting neutrals.

Subject headings: accretion, accretion disks — stars: planetary systems: protoplanetary disks — planets and satellites: formation — circumstellar matter — astrochemistry

1. INTRODUCTION

Transitional protostellar disks (hereafter TDs) are deficient in mid-infrared emission ($\lambda \lesssim 10\mu$m), implying a dearth of small dust grains interior to a few to several tens of AU (Skrutskie et al. 1990; Espaillat et al. 2014, and references therein). TDs are often supposed to represent an evolutionary stage intermediate between classical T Tauri systems, which have full disks, and weak-lined T Tauri systems, which have little or none. In this view, disks disperse from the inside out through some combination of photoevaporation, viscous evolution, and planet formation (Marsh & Mahoney 1992; Hollenbach et al. 1994; Clarke et al. 2001; Alexander et al. 2014, and references therein).

TDs tend to accrete less than full disks of comparable mass by factors $\sim$ 3-10 (Najita et al. 2015). The abundance of small dust in the disk cavity is suppressed by much larger factors (van der Marel et al. 2015). Some TDs, however, have accretion rates entirely comparable to those of full disks despite inner gaps of tens of AU (Manara et al. 2014). Evidently gas somehow crosses the gap between the outer disk and the star. Indeed, gas is detected within dust cavities of accreting TDs via H_2 fluorescence (Ingleby et al. 2009; Gorti et al. 2011) and rovibrational CO emission (Pontoppidan et al. 2008; Salyk et al. 2009). In both cases the emission appears to correlate with $\dot{M}$. Owen (2016) suggests that there are two types of TDs: (i) those that are faint at submillimeter wavelengths, have cavities $\lesssim 10\,\mathrm{AU}$, and accrete at $\dot{M} \lesssim 10^{-9}\,\mathrm{M_\odot\,yr^{-1}}$; (ii) those that are bright in the submillimeter, have cavities $\gtrsim 20\,\mathrm{AU}$, and accrete at $\sim 10^{-8}\,\mathrm{M_\odot\,yr^{-1}}$. The first type is consistent with expectations for photoevaporating disks, he suggests, whereas the latter is not. The present paper pertains mainly to class (i)—TDs that accrete rapidly despite large cavities.

The persistence of accretion suggests that within TD dust cavities either the ratio of small dust to gas is reduced, or the velocity of accretion is increased (implying a lower surface density for a given $\dot{M}$). Since quantitative measures of the gaseous surface density within TD cavities are sparse, many theoretical explanations for TDs have focussed on the former possibility, i.e. on mechanisms for altering the abundance of small grains per unit gas mass, such as photophoresis (Krauss & Wurm 2005), radiation pressure (Chiang & Murray-Clay 2007), pressure-induced dust filtering (Paardekooper & Mellema 2006; Rice et al. 2006; Zhu et al. 2012), or grain coagulation (Tanaka et al. 2005).

Alternatively or in combination with modified dust, mechanisms for increasing the radial speed of accretion ($v_{\rm acc}$) within TD cavities have been proposed. These include enhanced MRI turbulence (Chiang & Murray-Clay 2007; Suzuki et al. 2010) and planetary torques (Varnière et al. 2006; Zhu et al. 2011; Rosenfeld et al. 2014). At $\dot{M} \sim 10^{-8}\,\mathrm{M_\odot\,yr^{-1}}$, MRI alone cannot reduce the surface density below a few $\mathrm{g\,cm^{-2}}$ at relevant radii, which does not render the disk optically thin with standard ISM dust and would appear also to violate direct constraints on the gas column in some systems (§2.1). Planetary-torque models, even with multiple planets, have difficulty opening wide and clean gaps while still maintaining high accretion rates.

In this paper, we focus on a well-recognized mechanism that naturally produces rapid accretion: magnetized disk winds. Despite much work on disk winds since the seminal papers of Blandford & Payne (1982) and Pudritz (1985), applications to transitional disks have rarely been remarked upon. Notably however, Combet & Ferreira (2008) envisage a disk with relatively high surface density driven by turbulent viscosity at large radius, but with a lower wind-driven surface density within some transition radius r_J. Even in that paper, the term "transitional disk" appears only once in passing. The authors' motivation appears to have been mainly theoretical, having to do with inward concentration of large-scale poloidal magnetic flux brought about by competition between radial advection and turbulent diffusion. The radial redistribution of magnetic flux is a difficult problem (§2.3), and we

[1] Princeton University Observatory, Princeton, NJ 08544

are agnostic as to whether CF08's transition radius r_J can be predicted from first principles.

Our motivation for considering this type of model arose from other considerations. First, MRI-driven turbulence in active layers of disks with total surface densities comparable to the minimum-mass solar nebula seems only marginally viable at radii $\sim$ 1-10 AU: such turbulence requires field strengths approaching equipartition with the local gas pressure in order to reproduce observed accretion rates (Bai & Goodman 2009; Bai 2011). Secondly, recent numerical simulations of MRI turbulence with ambipolar diffusion often laminarize and produce spontaneous outflows (Bai & Stone 2013; Gressel et al. 2015). Thirdly, recent constraints derived from ALMA data on the gas content within the cavities of a few robustly accreting TDs demand accretion speeds at least as high as the gas sound speed (§2.1).

The outline of the paper is as follows. §2 summarizes the observational evidence for rapid inflow and the theoretical reasons for expecting wind-driven accretion to be transsonic. We also review the importance of ambipolar diffusion, at least under laminar conditions, for allowing the gas to accrete without overly concentrating the magnetic flux. This leads to a calculation in §3 of the expected degree of ionization and ambipolar coupling of the gas to the field in the cavity regions. It is found that ambipolar diffusion is plausibly in the Goldilocks range: neither so rapid as to undercut the magnetic wind torque on the neutrals, nor so slow as to cause the field to be accreted with the gas. We write "plausibly" because this is a complex calculation subject to many uncertainties in the chemical network, dust effects, and radiation field. §4 summarizes our findings and directions for future research.

2. DYNAMICAL CONSIDERATIONS

2.1. *Constraints on inflow speed*

If the surface density of gas in a TD dust cavity were known, then the inflow speed could be estimated from the observed accretion rate on the assumption of steady state. While gas has been detected in a number of TD cavities, the amount of gas has not often been reliably quantified. Bruderer (2013) has argued that CO should survive photodissociation even if the gas and dust surface densities are suppressed by several orders of magnitude. Rotational transitions trace the total gas content more reliably than rovibrational ones because of the lower excitation temperatures and critical densities of the former. ALMA has now made it possible to resolve TD cavities in CO rotational transitions. In a recent study, van der Marel et al. (2016, hereafter vdM16) have applied this method to four TDs, using multiple isotopologues of carbon monoxide (^{12}CO, ^{13}CO, C^{18}O) to correct for optical depth and photodissociation. Three of their four systems have quoted accretion rates $> 10^{-9}\,\mathrm{M_\odot\,yr^{-1}}$. Of these, DoAr44 is particularly interesting because the gas surface density (Σ) within 16 AU is inferred to be no more than $\sim 10^{-4}$ of an extrapolation from the outer disk. Specifically, in vdM16's model, $\Sigma(r) \lesssim 5\times10^{-3}\ r_{16}^{-1}$ g cm^{-2} for $r_{16} \equiv r/(16\,\mathrm{AU}) < 1$. Yet $\dot{M} = 9\times10^{-9}\,\mathrm{M_\odot\,yr^{-1}}$. The implied accretion speed is

$$v_{\rm acc} = \frac{\dot{M}}{2\pi r\Sigma} \gtrsim 0.8\,\mathrm{km\,s^{-1}}. \quad (1)$$

This is comparable to the sound speed if the hydrogen is molecular and its temperature is in equilibrium with the radiation field of the star ($T_{\rm eq} \approx 100\,r_{16}^{-1/2}$ K): $c_{\rm s} \approx 0.7 r_{16}^{-1/4}\,\mathrm{km\,s^{-1}}$. Unless Σ is much less than vdM16's upper bound, the accretion speed (1) is much less than free fall speed, $v_{\rm ff} \approx 12\,r_{16}^{-1/2}\,\mathrm{km\,s^{-1}}$. On the other hand, it is much larger than can be explained by "viscous" accretion mechanisms: the implied Shakura-Sunyaev viscosity parameter would have to be $\alpha = \dot{M}\Omega/3\pi c_{\rm s}^2\Sigma \gtrsim 8$. Similar conclusions follow for the other two of van der Marel et al. (2016)'s systems that show appreciable accretion, viz. HD135344B & IRS48: the accretion speed is superviscous ($\alpha > 1$) but consistent with being subsonic or transsonic.

2.2. *Wind-driven inflow*

Magnetized winds from thin disks naturally drive much faster accretion than "viscous" mechanisms that conserve the angular momentum within the disk, such as magnetorotational turbulence. This has been noted previously (e.g. Pelletier & Pudritz 1992), but because it often goes unremarked in works that focus on the launching or collimation of winds, the reasons are worth reviewing.

Consider an annular control volume $(z, r, \phi) \in [-h, +h] \times [r_1, r_2] \times [-\pi, \pi]$ in cylindrical coordinates aligned with the disk, which has half thickness $\sim h \ll r_1$. By integrating the mass flux $\rho\boldsymbol{v}$ and angular-momentum flux[2] $r(\rho v_\phi \boldsymbol{v} - B_\phi \boldsymbol{B}/4\pi)$ over the surface of this volume and assuming an axisymmetric statistical steady state, one easily sees that

$$\left[\dot{M}_a(r) j(r) + \frac{r}{2}\int_{-h}^{h} B_r B_\phi\, dz\right]_{r=r_1}^{r=r_2} = \int_{r_1}^{r_2}\left(\frac{d\dot{M}_w}{dr} j(r) - \frac{r^2}{2}\left[B_\phi B_z\right]_{z=-h}^{z=h}\right) dr,$$

in which $\dot{M}_a(r)$ is the total mass flow inward past radius r, $\dot{M}_w(r)$ is the total outflow of the wind from the disk surfaces ($z = \pm h$) within radius r, and $j(r) = r v_\phi \approx \sqrt{GM_* r}$ is the mean specific angular momentum at r. Noting that $d\dot{M}_a/dr = d\dot{M}_w/dr$ in steady state and taking $r_2 \to r_1$ leads to a differential statement of the conservation of angular momentum:

$$r^{-1}\dot{M}_a \frac{dj}{dr} = -h\overline{B_r B_\phi} - \tfrac{1}{2} r\left[(B_z B_\phi)^+ - (B_z B_\phi)^-\right], \quad (2)$$

where the overbar indicates a vertical average, and $B_i^\pm$ is shorthand for $B_i(r, \pm h)$.

Thus the advantage of winds over MRI turbulence in driving accretion is geometrical: the wind stress $B_z B_\phi$ acts on a surface area $\sim \pi r^2$, whereas the "viscous" $B_r B_\phi$ stress acts on a much smaller area $\sim 2\pi r h$. If the radial and vertical components of the magnetic field have comparable strength, then the former exert a torque larger than the latter by a factor $\sim r/h \sim \Omega r/c_{\rm s} \gg 1$. With

[2] We neglect Reynolds compared to Maxwell stresses, so that $\boldsymbol{v}$ can be replaced by its temporal and azimuthal mean.

the usual symmetry $(B_z, B_r, B_\phi)^+ = (B_z, -B_r, -B_\phi)^-$, the accretion speed becomes

$$v_{\rm acc} \approx -\frac{B_z B_\phi^+}{\pi \Sigma \Omega} \ . \tag{3}$$

If all three components of the field are comparable, then this becomes $v_{\rm acc} \approx V_{\rm A}^2/\Omega h$, where $V_{\rm A}^2 = B_z^2/4\pi\rho_0$ is the Alfvén speed based on conditions at the midplane, and $h \equiv \Sigma/2\rho_0$ is the effective half thickness of the disk. If this thickness is determined by a balance between gas pressure and the tidal field, then $\Omega h \sim c_{\rm s}$, so that the Mach number of accretion is $\sim (V_{\rm A}/c_{\rm s})^2$. Hence winds with near-equipartition fields should drive transsonic accretion.

In the semi-analytic wind models developed by Königl (1989), Wardle & Königl (1993), and Li (1996), $v_{\rm acc}$ is in fact typically comparable to the sound speed, or even a few times larger.[3] This is also true of numerical simulations that treat the disk structure explicitly and approach a steady state (Casse & Keppens 2002; Zanni et al. 2007a; Tzeferacos et al. 2009).

2.3. *Advection of flux*

Despite their greater efficiency at removing angular momentum from accreting matter, wind models are generally more complicated to use than turbulent/viscous ones. The magnetic geometry of the wind must be solved for globally, and the loading of the field lines with matter launched from the disk surface must be consistent with the physical state of the gas at that surface. Wind dynamics cannot easily be reduced to a single dimensionless parameter comparable to the Shakura-Sunyaev turbulent-viscosity parameter α.

In steady state, matter accreting through the disk must be able to cross field lines so that magnetic flux is not dragged with it. Otherwise, the radial concentration of flux will exert an outward force on the disk, producing subkeplerian rotation and possibly choking off the accretion or at least slowing it down (Bisnovatyi-Kogan & Ruzmaikin 1976; Narayan et al. 2003). Indeed, the tendency to subkeplerian rotation might prevent the formation of protostellar disks in the first place (Li et al. 2014, and references therein). The wind models of Königl and collaborators invoke ambipolar diffusion to separate the accreting neutral gas from the magnetic flux. This process is characterized by the ratio of the neutral-ion collision time to the orbital time,

$$\begin{aligned} {\rm Am} &\equiv \frac{\tau_{\rm ni}^{-1}}{\Omega} \\ &\sim 0.56 \ \left(\frac{n_e}{\rm cm^{-3}}\right) \left(\frac{r}{16 \ \ {\rm AU}}\right)^{3/2} \left(\frac{M_*}{M_\odot}\right)^{-1/2} \ . \end{aligned} \tag{4}$$

Here we have evaluated the parameter Am for the surface-density profile fitted by vdM16 to DoAr44. It will be shown in §3 that the electron density at the midplane within the disk cavity is plausibly such that Am $\sim$ 1-10.

The ambipolar drift velocity between the neutral and charged species when the latter are tied to the field is

$$\boldsymbol{v}_{\rm drift} \approx {\rm Am}^{-1} \frac{\boldsymbol{B}\times(\boldsymbol{\nabla}\times\boldsymbol{B})}{4\pi\rho\Omega} \ , \tag{5}$$

and $v_{\rm drift} \approx v_{\rm acc}$ if the field is stationary. The reduction in orbital velocity due to radial magnetic force is

$$\Delta v_\phi \approx \hat{\boldsymbol{e}}_r \cdot \frac{\boldsymbol{B}\times(\boldsymbol{\nabla}\times\boldsymbol{B})}{8\pi\rho\Omega} \ . \tag{6}$$

Hence $v_{{\rm drift},\,r}/\Delta v_\phi \approx 2{\rm Am}^{-1}$. In order that $v_{{\rm drift},\,r} \sim c_{\rm s}$ while $\Delta v_\phi \ll \Omega r$, it is therefore necessary that Am $\ll 2\Omega r/c_{\rm s} \sim 20$. On the other hand, Am $\gtrsim 1$ is needed for adequate coupling. We are not aware of a feedback mechanism to ensure that this rather narrow parameter range is realized at the midplane in the cavity.

Following the methods presented in §3.2, "fiducial" values of the radiation field and other physical parameters do indeed suggest that Am is in the desired range or close to it. However, this is likely not to be the last word on the subject because of the complex microphysics involved in the calculation and its sensitivity to input parameters such as the X-ray flux and dust abundance. *A priori*, if Am lies outside the desired range, it seems more likely to be too large than too small on the grounds that (i) surely Am $\gtrsim 1$ in the active layers of full disks and the outer parts of transitional disks, else no magnetic mechanism, whether relying on MRI or winds, could be effective in driving accretion there; and (ii) the lower surface density of the cavity gas and greater proximity to the sources of ionization might be expected to raise Am.

The problem of accretion of magnetic flux in ideal MHD is not new. When accretion is assumed to be driven by turbulent "viscosity", the concern is often opposite to that expressed here: namely, that turbulent diffusivity might allow the poloidal flux to escape too easily (van Ballegooijen 1989; Lubow et al. 1994; Spruit & Uzdensky 2005). In steady-state wind models based on near-ideal MHD, just enough turbulent diffusivity is invoked to allow the flux to be stationary as the gas accretes (Blandford & Payne 1982; Ferreira & Pelletier 1995; Zanni et al. 2007b, and references therein). The questions then become (i) What is the origin of the turbulence? (ii) How is the turbulent diffusivity regulated so that the magnetic flux neither accretes nor escapes?

A possible answer to question (i) above is MRI, whose turbulent diffusivity has been measured by several authors (Lesur & Longaretti 2009; Guan & Gammie 2009; Fromang & Stone 2009). But MRI tends to be inhibited or suppressed by poloidal fields as strong as are found in many wind models (Salmeron et al. 2007; Bai & Stone 2013; Gressel et al. 2015). If the field *were* to become too strong to allow MRI, it is unclear what instability would arise to cause that field to reconnect or diffuse so as to allow MRI to return: that is, we lack an answer to question (ii) above. Nonaxisymmetric interchange instabilities are possible but should occur only if $d(B_z/\Sigma)/dr < 0$, (Spruit et al. 1995; Stehle & Spruit 2001; Igumenshchev 2008), and while the interchange instability can rearrange the radial profile of B_z, it does not by itself alter B_z/Σ in a lagrangian sense. It may not be effective in reconnecting the horizontal components of magnetic field. More promising in this regard is the recently much-discussed plasmoid instability of cur-

[3] The horizontal components of field, which vanish at the midplane, compress the thickness h to less than its tidal value, strengthening the conclusion of the previous paragraph.

rent sheets (Loureiro et al. 2007; Loureiro & Uzdensky 2016), but this instability has not yet been studied in the presence of a field component perpendicular to the sheet (B_z here).

3. PHYSICAL STATE OF THE CAVITY GAS

As the discussion above makes clear, it is crucial to understand the degree of ionization of the gas in TD cavities. In this and in the following section, we assume a low surface density compatible with transsonic accretion, and then calculate the resulting ionization fraction, ohmic diffusivity, and ambipolar parameter.

3.1. *First estimate*

A simple analytic estimate of the electron density can be obtained by balancing X-ray ionization and radiative recombination of hydrogen. The surface density of the gas in the cavity is so low that we take it to be optically thin to the X-rays.

Recent observations of TDs indicate a typical X-ray luminosity $L_X \sim 10^{30}\,\mathrm{erg\,s^{-1}}$, and a characteristic photon energy ~ 1 keV (Kim et al. 2013). Balancing photoionization of molecular hydrogen against radiative recombination to atomic hydrogen (see Draine 2011), one obtains

$$n_e \sim 40\ \mathrm{cm^{-3}}\ \left(\frac{x_e}{3\times10^{-6}}\right)\left(\frac{r}{16\ \mathrm{AU}}\right)^{-2}\left(\frac{\langle h\rangle}{r}\right)^{-1}\ ,$$
$$x_e \sim 3\times10^{-6}\left(\frac{T}{10^2\ \mathrm{K}}\right)^{0.46}\left(\frac{\langle h\nu\rangle}{\mathrm{keV}}\right)^{-2}\ . \qquad (7)$$

This rough estimate would suggest that ambipolar diffusion is inefficient, i.e. Am $\gg 1$ in eq. (4). But the estimate neglects important recombination processes involving molecules and dust grains.

3.2. *Improved estimate: Method*

For a better estimate, we take into account multiple chemical species in addition to hydrogen, including a simplified treatment of dust grains, and far-UV (FUV) as well as X-ray ionization.

The calculations are done in spherical polar coordinates, dividing the gas into 100 radial zones spaced logarithmically in *cylindrical* radius from $r = 1\,\mathrm{AU}$ to $r = 50\,\mathrm{AU}$, and 20 latitudinal zones spaced linearly from $\theta = 0$ (midplane) to $\theta = 0.2$. Radiative transfer of the ionizing photons is calculated by integrating along radial rays, so that the calculations are effectively one-dimensional, except for some implicit scattering of the X-rays after they strike the disk surface. The surface mass density within the cavity is taken as $\Sigma \sim 5\times10^{-3}\ r_{16}^{-1}$ g cm^{-3} following §2.1. To allow for a finite angle between the ionizing rays and the disk surface [e.g. Perez-Becker & Chiang (2011)], we consider a flared disk with $h \propto r^{5/4}$ and $h = 0.1r$ at $r = 16\,\mathrm{AU}$ ($r_{16} = 1$). Hydrogen nuclei are distributed as

$$n_{\mathrm{H}}(r,z) = n_0 r_{16}^{-2.25}\exp[-(r\tan\theta)^2/(2h^2)]\ ,$$

with $n_0 = 10^{8\pm1}\,\mathrm{cm^{-3}}$. The gas is assumed vertically isothermal with radial temperature profile $T = T_0 r_{16}^{-1/2}$ and $T_0 = 100$ K, 30 K or 300 K.

Ionizing photons emanate from the origin $r = 0$ with total luminosities $L_X = 10^{30\pm1}$ erg s^{-1} and $L_{\mathrm{FUV}} = 10^{30\pm1}$ erg s^{-1}. FUV photons are taken to be monochromatic with $h\nu = 12\,\mathrm{eV}$ Extreme UV photons ($h\nu > 13.6\,\mathrm{eV}$) are ignored on the grounds that their penetration depths are negligible. Even FUV photons have rather little effect on the ionization balance at depth in the disk because of our restriction to purely radial propagation: The radial column density that must be crossed to reach the midplane at $r \gtrsim 1\,\mathrm{AU}$ is $N_{\mathrm{H_2}} \sim 10^{24}$ cm^{-2}, falling to $\sim 10^{22}$ cm^{-2} at 1-2 scale heights (h) off the plane.

X-ray penetration is calculated via the fit by Bai & Goodman (2009) to the Monte-Carlo results of Igea & Glassgold (1999), and hence implicitly includes some scattering and secondary effects. Following Bai & Goodman (2009), all ionizations are attributed to hydrogen and helium for the purpose of solving the chemical network; however, the total X-ray cross section per gram of gas takes into account a solar abundance of oxygen and other metals. X-ray photons are taken to be monochromatic with $h\nu = 3$ keV.

Time-dependent rate equations

$$\frac{\mathrm{d}x^i}{\mathrm{d}t} = \sum_{j,k} A^i{}_{jk}x^j x^k + \sum_j B^i{}_j x^j\ , \qquad (8)$$

are integrated to obtain the concentrations $\{x^i\}$ of the various species. The rate coefficients $\{A^i{}_{jk}\}$ of two-body reactions are taken from the `UMIST` astrochemistry database (McElroy et al. 2013), and the $\{B^i{}_j\}$ of photoionization and photodissociation reactions are caluculated with the schemes elaborated earlier in this section. Nine abundant elements (H, He, O, C, N, S, Si, Mg, and Fe) are included at IN06 abundances together with compounds totalling 175 species (following Table A.1 of Ilgner & Nelson 2006, with H^+ added).

Since grains can be important for electron mobility and recombination, the following reactions are included (X stands for atomic or molecular species)

- $\mathrm{X^+ + gr \to X + gr^+}$;
- $\mathrm{X^+ + gr^- \to X + gr}$;
- $e^- + \mathrm{gr \to gr^-}$;
- $e^- + \mathrm{gr^+ \to gr}$.

Higher grain charges are ignored because we assume small grains (see below). The rates of these reactions are estimated following Ilgner & Nelson (2006) and Bai & Goodman (2009), with reference to Draine & Sutin (1987) for collision rates and to Nishi et al. (1991) for electron sticking probabilities. We set the dust-to-gas mass ratio to $\sim 10^{-4}$, the density within grains to $3\,\mathrm{g\,cm^{-3}}$, and the grain radius to 10^{-3} μm. These choices bound the plausible area of grain surface from above, and hence lead to a conservative lower bound on n_e. Grain-assisted molecular hydrogen formation is estimated following the prescription of Bai & Goodman (2009).

Equations (8) are integrated to steady state cell by cell, ignoring advection of species between cells (except ionizing photons), because the local equilibration timescales are usually short compared to advection times, as discussed below (§3.3).

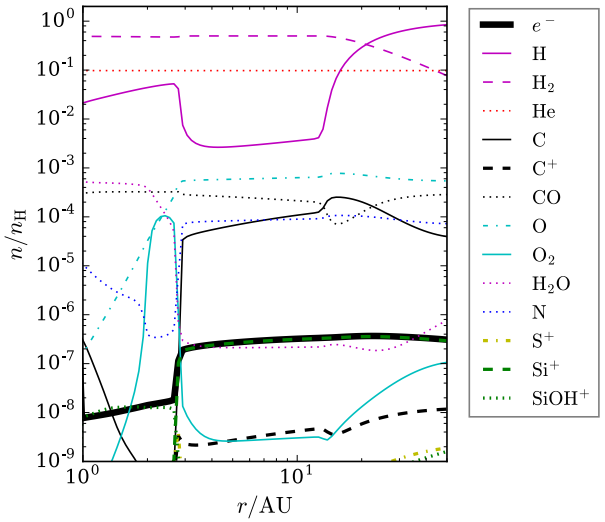

FIG. 1.— Relative abundance of significant neutral ($n/n_{\rm H} > 10^{-5}$) and ionic ($n/n_{\rm H} > 10^{-8}$) species. The relative abundance of electrons is shown by the heavy magenta curve; other species as noted in the legend.

TABLE 1
MODEL NUMBER AND PARAMETERS

Model No.	Description
0	Fiducial
1	No dust
2	$L_X = 10^{29}$ erg s^{-1}
3	$L_X = 10^{31}$ erg s^{-1}
4	$n_0 = 10^7$ cm^{-3}
5	$n_0 = 10^9$ cm^{-3}
6	$T_0 = 30$ K
7	$T_0 = 300$ K

3.3. *Second estimate: Results*

Figure 1 plots the abundance at the midplane ($\theta = 0$) of major species relative to hydrogen for the fiducial model, in which $L_X = L_{\rm FUV} = 10^{30}$ erg s^{-1}, $n_0 = 10^8$ cm^{-3}, $T_0 = 100$ K, and $r_{\rm dust} = 10^{-3}$ μm. The electron abundance depends depend rather weakly on radius, while the dominant positive ions are Si^+ and $SiOH^+$. Photoionization of helium and oxygen are competitive with that of molecular hydrogen as a source of free electrons.

For the fiducial case, the timescale on which n_e equilibrates is at least one order of magnitude shorter than the local accretion timescale $\tau_{\rm acc} \equiv r/v_{\rm acc}$ based on eq. (1), justifying our neglect of advection. This is not always true, however, especially in cases without dust.

We calculate seven additional models, each differing from the fiducial one in one parameter (Table 1). Following eq. (4), Fig. (2) exhibits the profiles of Am in the rz plane for all eight models.

The electron concentration and therefore Am increase as X-ray luminosity increases, and as density decreases: the latter is contrary to the trend for radiative hydrogen recombination and is due to molecular ions. The dependence on temperature is relatively complicated and subtle, as temperature affects the rates of radiative, dissociative and dust-assisted recombination in different ways. Comparison between Models 0 and 1 illustrates the importance of small dust. Eliminating dust-assisted recombination raises the electron density by one to two orders of magnitude.

The fiducial model has a relatively low-Am region that extends radially to ~ 3 AU, and vertically to 1-2 scale heights (h). Similar regions exist in Models 2, 5 and 7, and less clearly in Models 1 and 3. The exponential attenuation of X-rays with increasing column density actually lowers the ionization parameter $\xi \equiv \zeta/n_{\rm H}$ at smaller radii. The boundary of the low-Am regions corresponds to a transition in the dominant ion from Si^+ at relatively high n_e, to $SiOH^+$ (which has a larger dissociative-recombination cross section) at lower n_e.

We have used these results for the physical state of the gas to recompute the local wind model of Wardle & Königl (1993). As already noted, their model requires Am $\sim O(1)$ near the midplane, so that the coupling of the neutrals to the magnetic field is efficient enough to drive a wind but not so perfect as to accrete the magnetic flux. Fig. (2) shows that $0.3 \lesssim$ Am $\lesssim 30$ at $r \lesssim 10$ AU in most of our models, excepting those with rather high ionization parameter or without dust. Quantitatively, we find that the radial velocity of the neutral gas at the midplane varies from $\sim 10^{-1}$ to $\sim 10^0 c_s$, and the accretion rate from 10^{-9} to 10^{-8} $M_\odot$/yr. These latter are generally consistent with observed accretion rates in transitional disks.

4. DISCUSSION AND SUMMARY

We have seen that magnetized winds can rather naturally explain the combination of low gas and dust surface density and relatively robust accretion in transition-disk cavities. From a theoretical point of view, the suggestion is all the more natural because of previous work demonstrating the likelihood of *photoevaporative* winds on the one hand (Hollenbach et al. 1994; Clarke et al. 2001; Alexander et al. 2006; Owen et al. 2010), and the need for net poloidal magnetic flux to sustain magnetorotational turbulence in the minimally ionized parts of protostellar disks, on the other (Fleming et al. 2000; Oishi & Mac Low 2011; Flock et al. 2012; Bai & Stone 2011; Simon et al. 2013b,a). A thermally-driven outflow threaded by magnetic lines is bound to exert a torque on the gas remaining in the disk and drive some accretion, though just how much will require detailed modeling of a sort not attempted in the present work.

If the whole vertical column of the disk were to accrete at $v_{\rm acc} \sim c_{\rm s}$, then the surface density corresponding to observed accretion rates would be much less than what is inferred observationally, e.g. from submillimeter observations (Beckwith & Sargent 1993; Andrews et al. 2013). Thus in the parts of TDs exterior to their cavities, as well as in full (non-transitional) T Tauri disks, either accretion is driven turbulently (and hence relatively slowly), or else it is again driven by a magnetized wind, but one that couples to only a small fraction of the vertical column where FUV and X-ray photons sufficiently ionize and heat the gas (Bai 2016).

Not addressed here is the *cause* of the transition between slow/layered accretion at large radii and fast, wind-driven, full-column accretion within the cavity. Perhaps, as proposed by Combet & Ferreira (2008), this has to do with a critical value of magnetization brought about by advection of poloidal flux. But as discussed

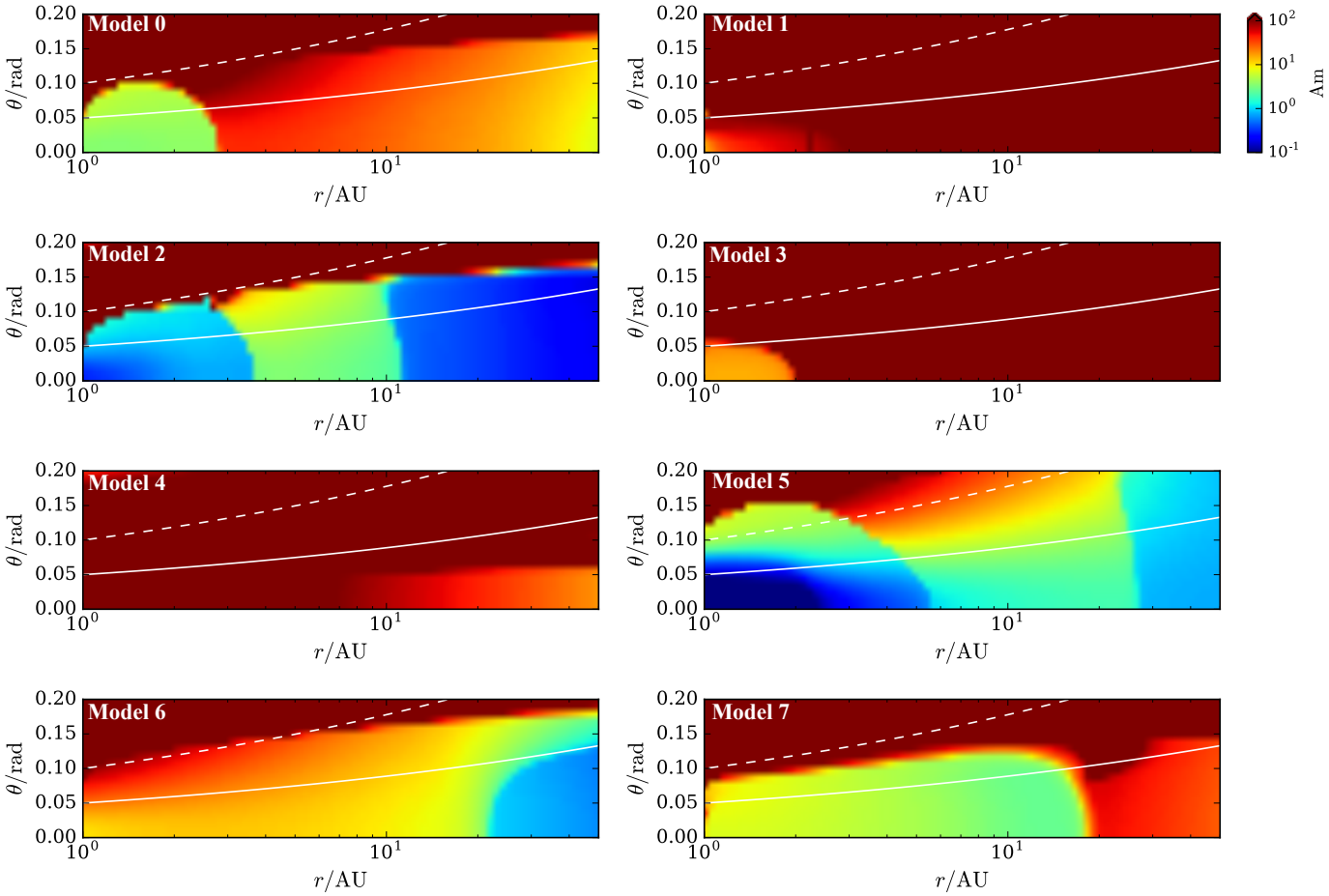

FIG. 2.— Ambipolar parameter Am vs. cylindrical radius r and latitude θ. Each panel corresponds to one of the models in Table 1, as marked. White curves are loci of constant gaussian scale height: h (solid), and $2h$ (dashed).

in §2.3, the advection and diffusion of magnetic flux in a turbulent disk is an unsolved problem. Also, if this is the explanation, why aren't all T Tauri disks transitional? Perhaps indeed giant planets are implicated, but rather than producing the entire cavity by gravitational torques alone, such planets trigger a local change in the mass-to-flux ratio by stemming the inflow of gas near the midplane (which feels little magnetic torque) but not the inflow of the more ionized surface layers (which are more strongly magnetically driven, whether by winds or MRI). In any case, one should entertain the possibility that transitional disks—or at least those that have accretion rates comparable to those of full disks—may not be an evolutionary phase that all disks pass through immediately before complete dispersal.

This work was supported by NASA Origins of Solar Systems grant NNX10AH37G.

REFERENCES

Alexander, R., Pascucci, I., Andrews, S., Armitage, P., & Cieza, L. 2014, Protostars and Planets VI, 475
Alexander, R. D., Clarke, C. J., & Pringle, J. E. 2006, MNRAS, 369, 216
Andrews, S. M., Rosenfeld, K. A., Kraus, A. L., & Wilner, D. J. 2013, ApJ, 771, 129
Bai, X.-N. 2011, ApJ, 739, 50
—. 2016, ApJ, 821, 80
Bai, X.-N., & Goodman, J. 2009, ApJ, 701, 737
Bai, X.-N., & Stone, J. M. 2011, ApJ, 736, 144
—. 2013, ApJ, 769, 76
Beckwith, S. V. W., & Sargent, A. I. 1993, in Protostars and Planets III, ed. E. H. Levy & J. I. Lunine, 521–541
Bisnovatyi-Kogan, G. S., & Ruzmaikin, A. A. 1976, Ap&SS, 42, 401
Blandford, R. D., & Payne, D. G. 1982, MNRAS, 199, 883
Bruderer, S. 2013, A&A, 559, A46
Casse, F., & Keppens, R. 2002, ApJ, 581, 988
Chiang, E., & Murray-Clay, R. 2007, Nature Physics, 3, 604
Clarke, C. J., Gendrin, A., & Sotomayor, M. 2001, MNRAS, 328, 485
Combet, C., & Ferreira, J. 2008, A&A, 479, 481
Draine, B. T. 2011, Physics of the Interstellar and Intergalactic Medium (Princeton University Press)
Draine, B. T., & Sutin, B. 1987, ApJ, 320, 803
Espaillat, C., Muzerolle, J., Najita, J., et al. 2014, Protostars and Planets VI, 497
Ferreira, J., & Pelletier, G. 1995, A&A, 295, 807
Fleming, T. P., Stone, J. M., & Hawley, J. F. 2000, ApJ, 530, 464
Flock, M., Henning, T., & Klahr, H. 2012, ApJ, 761, 95
Fromang, S., & Stone, J. M. 2009, A&A, 507, 19
Gorti, U., Hollenbach, D., Najita, J., & Pascucci, I. 2011, ApJ, 735, 90
Gressel, O., Turner, N. J., Nelson, R. P., & McNally, C. P. 2015, ApJ, 801, 84
Guan, X., & Gammie, C. F. 2009, ApJ, 697, 1901
Hollenbach, D., Johnstone, D., Lizano, S., & Shu, F. 1994, ApJ, 428, 654
Igea, J., & Glassgold, A. E. 1999, ApJ, 518, 848
Igumenshchev, I. V. 2008, ApJ, 677, 317
Ilgner, M., & Nelson, R. P. 2006, A&A, 445, 205
Ingleby, L., Calvet, N., Bergin, E., et al. 2009, ApJ, 703, L137

Kim, K. H., Watson, D. M., Manoj, P., et al. 2013, ApJ, 769, 149
Königl, A. 1989, ApJ, 342, 208
Krauss, O., & Wurm, G. 2005, ApJ, 630, 1088
Lesur, G., & Longaretti, P.-Y. 2009, A&A, 504, 309
Li, Z.-Y. 1996, ApJ, 465, 855
Li, Z.-Y., Banerjee, R., Pudritz, R. E., et al. 2014, Protostars and Planets VI, 173
Loureiro, N. F., Schekochihin, A. A., & Cowley, S. C. 2007, Physics of Plasmas, 14, 100703
Loureiro, N. F., & Uzdensky, D. A. 2016, Plasma Physics and Controlled Fusion, 58, 014021
Lubow, S. H., Papaloizou, J. C. B., & Pringle, J. E. 1994, MNRAS, 267, 235
Manara, C. F., Testi, L., Natta, A., et al. 2014, A&A, 568, A18
Marsh, K. A., & Mahoney, M. J. 1992, ApJ, 395, L115
McElroy, D., Walsh, C., Markwick, A. J., et al. 2013, A&A, 550, A36
Najita, J. R., Andrews, S. M., & Muzerolle, J. 2015, MNRAS, 450, 3559
Narayan, R., Igumenshchev, I. V., & Abramowicz, M. A. 2003, PASJ, 55, L69
Nishi, R., Nakano, T., & Umebayashi, T. 1991, ApJ, 368, 181
Oishi, J. S., & Mac Low, M.-M. 2011, ApJ, 740, 18
Owen, J. E. 2016, PASA, 33, e005
Owen, J. E., Ercolano, B., Clarke, C. J., & Alexander, R. D. 2010, MNRAS, 401, 1415
Paardekooper, S.-J., & Mellema, G. 2006, A&A, 453, 1129
Pelletier, G., & Pudritz, R. E. 1992, ApJ, 394, 117
Perez-Becker, D., & Chiang, E. 2011, ApJ, 735, 8
Pontoppidan, K. M., Blake, G. A., van Dishoeck, E. F., et al. 2008, ApJ, 684, 1323
Pudritz, R. E. 1985, ApJ, 293, 216
Rice, W. K. M., Armitage, P. J., Wood, K., & Lodato, G. 2006, MNRAS, 373, 1619
Rosenfeld, K. A., Chiang, E., & Andrews, S. M. 2014, ApJ, 782, 62
Salmeron, R., Königl, A., & Wardle, M. 2007, MNRAS, 375, 177
Salyk, C., Blake, G. A., Boogert, A. C. A., & Brown, J. M. 2009, ApJ, 699, 330
Simon, J. B., Bai, X.-N., Armitage, P. J., Stone, J. M., & Beckwith, K. 2013a, ApJ, 775, 73
Simon, J. B., Bai, X.-N., Stone, J. M., Armitage, P. J., & Beckwith, K. 2013b, ApJ, 764, 66
Skrutskie, M. F., Dutkevitch, D., Strom, S. E., et al. 1990, AJ, 99, 1187
Spruit, H. C., Stehle, R., & Papaloizou, J. C. B. 1995, MNRAS, 275, 1223
Spruit, H. C., & Uzdensky, D. A. 2005, ApJ, 629, 960
Stehle, R., & Spruit, H. C. 2001, MNRAS, 323, 587
Suzuki, T. K., Muto, T., & Inutsuka, S.-i. 2010, ApJ, 718, 1289
Tanaka, H., Himeno, Y., & Ida, S. 2005, ApJ, 625, 414
Tzeferacos, P., Ferrari, A., Mignone, A., et al. 2009, MNRAS, 400, 820
van Ballegooijen, A. A. 1989, in Astrophysics and Space Science Library, Vol. 156, Accretion Disks and Magnetic Fields in Astrophysics, ed. G. Belvedere, 99–106
van der Marel, N., van Dishoeck, E. F., Bruderer, S., et al. 2016, A&A, 585, A58
van der Marel, N., van Dishoeck, E. F., Bruderer, S., Pérez, L., & Isella, A. 2015, A&A, 579, A106
Varnière, P., Blackman, E. G., Frank, A., & Quillen, A. C. 2006, ApJ, 640, 1110
Wardle, M., & Königl, A. 1993, ApJ, 410, 218
Zanni, C., Ferrari, A., Rosner, R., Bodo, G., & Massaglia, S. 2007a, A&A, 469, 811
—. 2007b, A&A, 469, 811
Zhu, Z., Nelson, R. P., Dong, R., Espaillat, C., & Hartmann, L. 2012, ApJ, 755, 6
Zhu, Z., Nelson, R. P., Hartmann, L., Espaillat, C., & Calvet, N. 2011, ApJ, 729, 47